

An analysis of hydrophobic interactions of thymidylate synthase with methotrexate: Free energy calculations involving mutant and native structures bound to methotrexate

Ramireddy Nageswara Reddy ·
Ravichandra Reddy Mutyala · Polamarasetty Aparoy ·
Pallu Reddanna · Mutyala Rami Reddy

Received: 27 January 2009 / Accepted: 6 May 2009 / Published online: 28 June 2009
© Springer-Verlag 2009

Abstract Since the human body for many reasons can adapt and become resistant to drugs, it is important to develop and validate computer aided drug design (CADD) methods that could help predict binding affinity changes that can result from these resistant enzymes. The free energy perturbation (FEP) methodology is the most accurate means of estimating relative binding affinities between inhibitors and protein variants. In this paper, we describe the role played by hydrophobic residues lining the active site region, particularly ⁷⁹Ile and ¹⁷⁶Phe, in the binding of methotrexate to the *Escherichia coli* (*E. coli*) thymidylate synthase (TS) enzyme, using the thermodynamic cycle perturbation (TCP) approach. The computed binding free energy differences on the binding of methotrexate to the native and some mutant *E. coli* TS structures

have been compared with experimental results. Computationally, four different ‘mutations’ have been simulated on the TS enzyme with methotrexate (MTX): ⁷⁹Ile→⁷⁹Val; ⁷⁹Ile → ⁷⁹Ala; ⁷⁹Ile → ⁷⁹Leu; and ¹⁷⁶Phe→¹⁷⁶Ile. The calculated results indicate that in each of these cases, the native residues (⁷⁹Ile and ¹⁷⁶Phe) interact more favorably with methotrexate than the mutant residues and these results are corroborated by experimental measurements. Binding preference to wild type residues can be rationalized in terms of their better hydrophobic contacts with the phenyl ring of methotrexate.

Keywords Double topology method · Methotrexate · MD simulations · Mutants · Relative binding free energies · Single topology method · Thymidylate synthase

R. N. Reddy · R. R. Mutyala
Rational Labs Pvt. Limited,
Plot #177, IDA Mallapur,
Hyderabad 500 076, India

R. R. Mutyala · M. R. Reddy
RR Labs Inc.,
8013 Los Sabalos Street,
San Diego, CA 92126, USA

P. Aparoy · P. Reddanna
School of Life Sciences, University of Hyderabad,
Hyderabad 500 046, India

M. R. Reddy (✉)
Metabasis Therapeutics Inc.,
11119 North Torrey Pines Road,
La Jolla, CA 92037, USA
e-mail: drmrreddy@yahoo.com

Introduction

Thymidylate synthase (TS) has emerged as an important therapeutic target for design of anti-metabolites with potential clinical efficacy against various proliferative and infectious diseases. The crystal structure of an *Escherichia coli* (*E. coli*) thymidylate synthase (TS) [1] ternary complex containing 5-fluoro-2'-deoxyuridylate (FdUMP) and 10-propargyl-5,8-dideazafolate (PDDF) was determined and refined at 2.3 Å resolution. Thymidylate synthase is a dimeric protein with molecular weight of 71 kD, that catalyzes the formation of 2'-deoxythymidylate (dTMP) from 2'-deoxyuridylate (dUMP) using 5,10-methylenetetrahydrofolate (CH₂-H₄PteGlu) as the source of the single carbon unit as well as the reductant. This one carbon transfer reaction is critical to cell division since it provides

the sole *de novo* source of dTMP for DNA synthesis. TS has activated dUMP and 5,10-methylenetetrahydrofolate [1] ($\text{CH}_2\text{-H}_4\text{PteGlu}$) leading to the formation of the intermediate and offers additional support for the hypothesis that the substrate and cofactor are linked by a methylene bridge between C-5 of the substrate nucleotide and N-5 of the cofactor. By correlating these structural results with the known stereo-specificity of the TS-catalyzed reaction, it can be inferred that the catalytic intermediate, once formed, must undergo a conformational isomerization before eliminating across the bond linking C-5 of dUMP to C-11 of the cofactor. The elimination itself may be catalyzed by proton transfer to the cofactor's 5 nitrogen from invariant Asp169 buried deep in the TS active site. TS inhibition interrupts the *de novo* synthesis of thymidylate from deoxyuridylate, which is crucial for DNA synthesis in cells [2–4]. Inhibition of TS has been achieved with analogs of both the folate cofactor and the pyrimidine substrate [1]. Inhibitors that bind at the folate site have attracted renewed attention, which resulted in strong TS binding to N-10-substituted 5,8-didecazafoolic acids. Most notable among the pyrimidines is the potent anti-tumor agent 5-fluoro-2'-deoxyuridylate (FdUMP), a metabolite of the anti-pyrimidines 5-fluorouracil and 5-fluorodeoxyuridine. Thus, rapid proliferation of cells can be arrested by the inhibition of TS, the rate-limiting step in the *de novo* pathway to thymidine nucleotides. Consequently, a large number of inhibitors of TS have been designed, synthesized, biochemically tested and in some of these cases, their complexes with the enzyme have also been studied by X-ray crystallography [1, 5]. The drug design paradigm involving iterative protein crystallographic analysis, computer design, synthesis and biochemical testing of TS inhibitors has been described [1]. In that study, *E. coli* ternary complex was used as a surrogate receptor for the iterative design of human TS inhibitors because of the abundance of the *E. coli* enzyme for experimental purposes and because of the conservation of over 75% of the active site residues at the folate binding site in *E. coli* and human TS structures. The crystal structure of the TS-dUMP complex [6, 7] shows that the completely conserved residue Asp-229 contributes the only side chain in direct hydrogen bonding with the pyrimidine ring of the substrate dUMP. In the binary and ternary complexes, the carboxamide moiety of the side chain of N229 forms a cyclic hydrogen bond network bridging N-3 and O-4 of the uracil heterocycle. Wild-type TS binds dCMP weakly and does not accept dCMP as a substrate. Mutations at N229 of TS modify the interaction of TS with dCMP.

Computer aided drug design (CADD) has been used successfully for the discovery of several novel enzyme inhibitors, including inhibitors of thymidylate synthase [8], HIV-1 protease [9, 10], purine nucleoside phosphorylase

[11] and fructose 1,6-bisphosphatase [12, 13]. The most accurate computational method for estimating relative binding affinities of structurally similar inhibitors to an enzyme is the free energy perturbation (FEP) approach using either molecular dynamics (MD) or Monte Carlo (MC) simulations [14]. Despite its high accuracy, free energy perturbation (FEP) calculations have primarily been used to rationalize experimentally-determined binding affinities [15–18] with few applications focusing on predictions [19–22]. Rational design of inhibitors for TS is also facilitated by the theoretical approaches which predict binding free energy differences for similar ligands which bind to the same active site. Earlier free energy perturbation calculations in this regard have rationalized the preferential binding of 10-propargyl-5,8-dideazafoolate relative to 10-formyl-5,8-dideazafoolate to the *E. coli* TS enzyme [23–25]. Reddy *et al.* [25] calculated the relative free energies for the closely related inhibitors 10-propargyl-5,8-dideazafoolic acid (PDDF) and 10-formyl-5,8-dideazafoolate (FDDF), binding to the binary complex consisting of the enzyme *E. coli* TS and 5-fluoro-2'-deoxyuridylate (FdUMP). The calculated relative binding free energy ($\Delta\Delta G_{\text{bind}}$), $2.9 \text{ kcal mol}^{-1}$, is in good agreement with the experimentally observed $3.75 \text{ kcal mol}^{-1}$ preference for PDDF. PDDF is more difficult for desolvation than FDDF, but the favorable interactions in the complex more than compensate for the desolvation costs. These investigations found that the propargyl moiety of PDDF interacts with a backbone carbonyl of the synthase and makes good hydrophobic contacts with side chain atoms.

Peter Kollman *et al.* [26] calculated the relative free energies of binding for dUMP and dCMP to TS and two Asn229 mutants using AMBER 4.0, the all-atom force field, and the TS-dUMP complex crystal structure. The calculated relative binding free energy of dUMP and dCMP with TS was analyzed as the sum of two components, the relative free energy difference of these two ligands in solvent water and the relative free energy difference in the protein complex. The results suggested that the TS.dCMP binary complex is inherently less stable than the TS.dUMP binary complex due to repulsive interactions between dCMP and the Asn229 side chain. Lee and Kollman [27] applied the free energy calculations using AMBER and PROFEC program to the design and evaluation of potential TS inhibitors with the goal of finding inhibitors that are selective for pathogen or cancer isozymes. Recently, Reddy *et al.* [28] calculated the relative binding affinities of Fructose-1,6-bis-phosphatase (FBPase) mutants with adenosine monophosphate (AMP) through free energy perturbation (FEP) method. The calculated relative binding free energy results for the mutations, $^{113}\text{Tyr} \rightarrow ^{113}\text{Phe}$, $^{31}\text{Thr} \rightarrow ^{31}\text{Ala}$, $^{31}\text{Thr} \rightarrow ^{31}\text{Ser}$, $^{177}\text{Met} \rightarrow ^{177}\text{Ala}$, and $^{30}\text{Leu} \rightarrow ^{30}\text{Phe}$ are in agreement with the experimental results.

The success of the FEP approach in rationalizing binding preferences of FBPase mutants has led us to employ the FEP methodology to better understand the role of hydrophobic residues at the active site of human TS. Earlier, several series of multiple mutants of *E. coli* TS have been generated. For methotrexate (MTX), a well-known inhibitor of the ligand, binding affinities have also been measured for several mutants of the *E. coli* TS enzyme. These mutations have an important role in the enzyme activity and this is the reason why drugs fail to work effectively for a long period on a particular disease. Hence, knowledge on the effect of mutations on the activity of the enzyme helps in the design of efficient and more potent drugs. In the light of the above concept, studies were taken up to further validate the FEP methodology for the calculation of the relative binding free energy differences for pairs of mutant and wild-type structures of the enzyme and compare the free energy results with experimentally determined binding affinities reported in the literature.

Materials and methods

Thermodynamic-cycle perturbation approach

The thermodynamic cycle-perturbation (TCP) approach (Fig. 1) is a method for computing the relative changes of binding free energy using non-physical paths connecting the desired initial and terminal states. This approach enables calculation of the relative change in binding free energy difference ($\Delta\Delta G_{\text{bind}}$) between two related TS mutants, by computationally simulating the ‘mutation’ of one to the other. The relative solvation free energy change between wild type and mutant of TS is computed using the following equation (Fig. 1):

$$\Delta\Delta G_{\text{sol}} = \Delta G_{\text{aq}} - \Delta G_{\text{gas}} \quad (1)$$

The relative binding free energy change between wild type and mutant of TS is computed using the (Fig. 1) following equation:

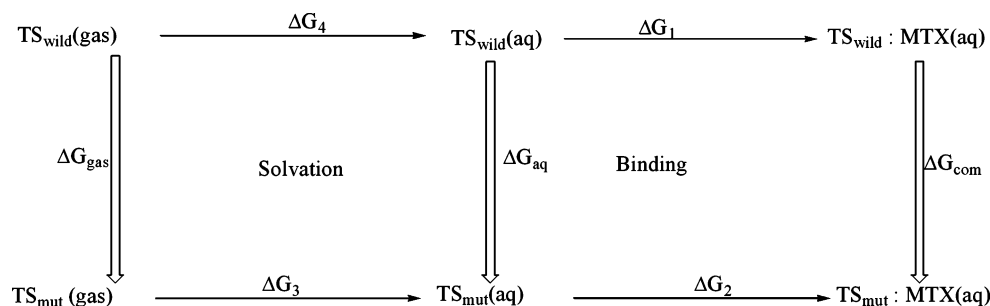
$$\Delta\Delta G_{\text{bind}} = \Delta G_{\text{com}} - \Delta G_{\text{aq}} = -k_{\text{B}}T \ln(k_2/k_1) \quad (2)$$

where k_{B} is the Boltzmann constant, T is the absolute temperature, and k_1 and k_2 refer to the experimentally

measured binding constants for wild type (TS(W):MTX) and mutant (TS(M):MTX) complexes respectively. The free energy change for converting wild type into mutant is computed by perturbing the Hamiltonian of reactant (initial) state TS(W) into that of the product (final) state TS (M). This transformation is accomplished through a parameterization of terms comprising the interaction potentials of the system with a change of state variable that maps onto reactant and product states when that variable is 0 and 1, respectively. The total free energy change for the mutation from the initial to the final state is computed by summing ‘incremental’ free energy changes over several windows visited by the state variable changing from 0 to 1. This approach enables calculation of the relative change in binding free energy difference between two related compounds by computationally simulating the ‘mutation’ of one to the other. The relative solvation and binding free energy changes for the two TS mutants with MTX inhibitor is computed using either single or double topology method.

A double topology [8, 24, 25] or thread method (Fig. 2) is used for large changes in mutations such as $^{176}\text{Phe} \rightarrow ^{176}\text{Ile}$ and a single topology (Fig. 3) is used for small changes in the mutations such as $^{79}\text{Ile} \rightarrow ^{79}\text{Val}$. In the thread method, for the amino acid residues which are mutated, both the starting and ending topologies are defined with their correct geometries, one beginning the simulation entirely as dummy atoms and the other ending the simulation entirely as dummy atoms. Dummies are topologically connected to real atoms, but have no charges or van der Waals parameters associated with them. At intermediate points of the non-physical transformation, all atoms of both topologies have fractional Lennard-Jones parameters and charges and interact simultaneously with the environment, but not with each other. The main advantage of this double topology method over the more commonly used single topology method is that it does not require direct ‘mapping’ of the reactant atoms to the product atoms and is thus more appropriate to treat mutations such as **Phe** \rightarrow **Ile**, involving residues which are topologically and chemically distinct. The transformations were achieved using the window method as implemented in the Galaxy program [29] and a two-stage procedure previously shown to enhance convergence [8].

Fig. 1 TCP cycle for calculating binding affinities of thymidylate synthase complexed with methotrexate



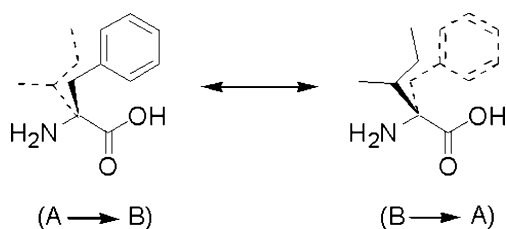


Fig. 2 Molecular threading of Phenylalanine (molecule A) and Isoleucine (molecule B). Common atoms are the atoms of the amino acid backbone. The non-common atoms are the side chain atoms which for $\lambda=0$ are real atoms for molecule A and dummy atoms for molecule B (dashed structure). At the completion of the transformation ($\lambda=1$), the side chain atoms for molecules A are dummy atoms and for molecule B are real atoms

In the first stage, the atomic charges of molecule A (the starting topology consisting of real atoms) were slowly turned off while the Lennard-Jones parameters of the atoms of molecule B (the starting topology consisting of dummy atoms) were slowly turned on. During the second stage, the Lennard-Jones parameters of molecule A were turned off while the charges of molecule B were turned on. In each stage, the transformation occurred over a total of 21 windows with each window consisting of 4.0 ps and 16.0 ps for equilibration and data collection, respectively for each mutation. Thus, each mutation required 860 ps of molecular dynamics simulation length to complete the mutation between two amino acid residues.

Force field parameters

All molecular dynamics and FEP calculations were performed with the AMBER program using an all atom force field [30, 31] and the SPC/E model potential [32, 33] to describe water interactions. The SPC/E water model, which provides a density, diffusion constant, and dielectric constant in excellent agreement with experiment, was chosen. This potential reproduces pertinent properties of bulk water quite well. Electrostatic charges and parameters for the TS wild type mutant residues were taken from the AMBER database. For methotrexate (Fig. 4), the partial charges were obtained by fitting wave functions calculated with Gaussian 98 program [34] and HF/ 6-31G* basis set

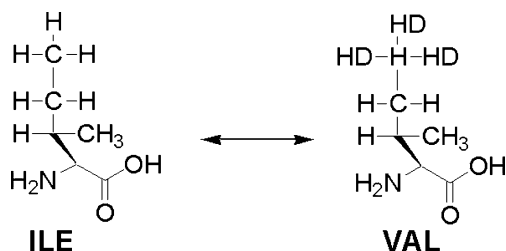


Fig. 3 Single topology definition of Ile and Val. The chemical definition with “D” prefix indicate dummy atoms

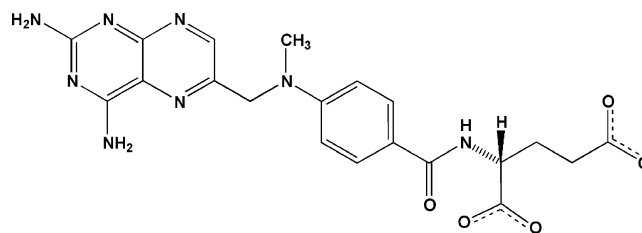


Fig. 4 Structure of methotrexate

level with CHELPG [35]. All equilibrium bond lengths, bond angles, and dihedral angles for nonstandard residues of methotrexate were taken from *ab initio* optimized geometries. Missing force field parameters were estimated from similar chemical species within the AMBER database. The hydrogens of the crystallographic water, the inhibitor and the protein dimer were added using the EDIT module of AMBER.

System setups for solvent and complex simulations

Relative solvation ($\Delta\Delta G_{\text{sol}}$) and relative binding ($\Delta\Delta G_{\text{bind}}$) free energies for mutants complexed to thymidylate synthase were calculated using the thermodynamic cycle perturbation (TCP) approach in conjunction with molecular dynamics (MD) simulations. The protein, the inhibitor and the solvent water were modeled using the AMBER all-atom force field. The AMBER Hamiltonian consists of energy contributions from bond length, bond angle and dihedral angle changes from equilibrium geometry, as well as van der Waal's, electrostatic and hydrogen bond interactions. All molecular dynamics (MD) simulations were performed using the AMBER program, employing standard MD techniques: the use of Verlet algorithm [36] for integrating the equations of motion with a 2 fs time step and the SHAKE option [37] was used for constraining all bond lengths. Constant temperature ($T=298$ K) is maintained by velocity scaling and a residue based cutoff of 15.0 Å was used for non-bonded interactions. However, all interactions among the solute atoms and atoms of the charged residues were included regardless of distance. Protein atoms beyond 25.0 Å from the center of the mutating groups were frozen. The protein was immersed in a 26.0 Å sphere of solvent centered at the same point and solvent molecules were subjected to a half-harmonic restraint near the boundary to prevent solvent evaporation.

In each simulation, the system was initially equilibrated for 20 ps followed by 4 ps of equilibration and 16 ps of data collection for each window. A total of 21 windows and 840 ps of MD simulations were used for each complete mutation. Error bars are estimated for each window by dividing the window statistics into eight groups and computing the standard deviation. The root mean square of these errors is reported in Table 1 as a measure of statistical uncertainty in the results for each complete

Table 1 Relative solvation and binding free energies in kcal mol⁻¹

S.No.	Mutation	$\Delta\Delta G_{\text{sol}}$	$\Delta\Delta G_{\text{bind}}$	$\Delta\Delta G_{\text{expt}}^c$
1	⁷⁹ Ile→ ⁷⁹ Val	-0.50±0.4	0.80±0.55	0.55
2	⁷⁹ Ile→ ⁷⁹ Ala	-0.60±0.4	1.80±0.50	1.40
3	⁷⁹ Ile→ ⁷⁹ Leu	-0.40±0.4	1.20±0.55	0.95
4 ^a	¹⁷⁶ Phe→ ¹⁷⁶ Ile	2.90±0.7	1.70±0.80	1.20
5 ^b	¹⁷⁶ Phe→ ¹⁷⁶ Ile	2.80±0.4	1.65±0.50	1.20

^a The relative binding free energy was calculated using 4 ps for equilibration and 16 ps for data collection in each window using 21 windows

^b The relative binding free energy was calculated using 8 ps for equilibration and 32 ps for data collection in each window using 21 windows

^c Experimental data. Villafranca JE, Matthews DA (unpublished data)

mutation. In order to understand the dependence of error bars on the length of MD simulation, we have calculated relative binding free energies between ¹⁷⁶Phe : MTX → ¹⁷⁶Ile : MTX using 840 ps and 1680 ps (8 ps of equilibration and 32 ps of data collection in each window for 21 windows) of MD simulations and compared the error bars between these two simulations. The calculated results (Table 1) indicated that error bars were reduced significantly when the simulation length is doubled and the changes in the final relative binding free energies between the mutants (1.70 kcal mol⁻¹ vs. 1.65 kcal mol⁻¹) is not significant. Therefore, the error bars will depend upon the length of the MD simulation significantly, but not the relative free energies.

Structural analysis

The starting point for our simulations is a high resolution (2.0 Å) structure of the *E. coli* TS enzyme. The protonation state of the histidines at the ring nitrogens inferred was deduced from hydrogen bonding and electrostatic interactions in the vicinity of the amino acid residue. As described in our earlier work [23], a bias toward protonation of both histidine nitrogens was applied in order to reduce the net charge on each monomer of the dimeric enzyme to -4e. These simulations do not employ counter ions. While such an electrostatic model has limitations, it is emphasized that our focus is on relative free energy differences due to ‘mutations’ in hydrophobic side chains. In addition, we used infinity cutoff for all non-bonded interactions between charged residues and the inhibitor (MTX) to eliminate any cutoff effects on the final results. We also, measured the residence times for a few charged and neutral residues in the binding site and noticed no significant differences between charged and neutral residues movements. In order to check the fidelity of the structure during MD calculations, a comparison of the X-ray structure has been made

with an average structure computed from a 20 ps trajectory of molecular dynamics calculations collected after a 20 ps equilibration of the minimized TS (wild-type) : MTX complex. RMS deviations of 1.1 Å and 1.8 Å are obtained for the main chain and side chain atoms respectively.

Results and discussion

The crystal structure TS:MTX complex provides the information regarding hydrophilic and hydrophobic residues (Fig. 5) in the binding site, but fails to reveal information regarding their relative contributions to binding affinity. This is true for hydrogen bonds whose strength varies from 2 to 4 kcal mol⁻¹ depending on the bond distance and bond angle, as well as the electronic nature of the donor and acceptor groups. In addition, the local environment is often an important factor with the strongest hydrogen bonds formed in poorly solvated regions of the binding site cavity. Since the contribution of individual hydrogen bonds to ligand binding affinity is considered valuable information for the design of new inhibitors, analogues of the lead inhibitor are frequently prepared wherein the individual heteroatoms that form hydrogen bonds with the protein are replaced with non-hydrogen bonding atoms or substituents. For similar reasons, site-directed mutagenesis is often used to replace binding site residues containing side-chains that interact with the inhibitor through a hydrogen bond with residues whose side-chains are incapable of forming hydrogen bonds. Data generated from the analogues and site-directed mutants can be used to determine the role of specific binding site

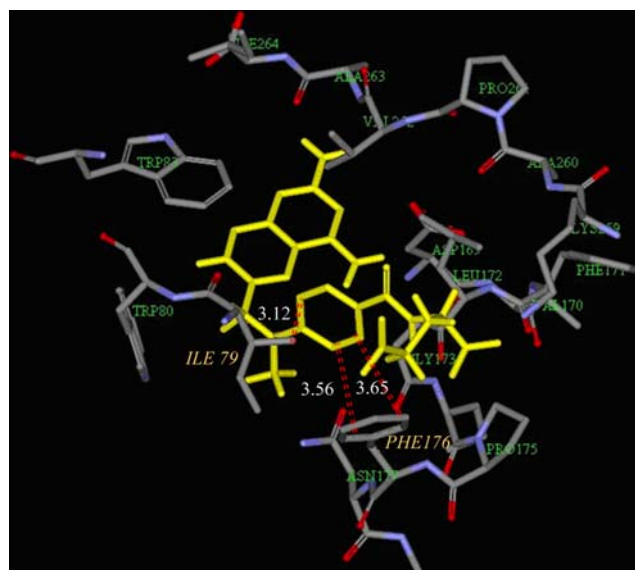


Fig. 5 Hydrophobic interactions of amino acids Ile-79 and Phe-176 with methotrexate (shown in yellow). The amino acid residues within 10 Å are shown (bond distance Å)

interactions in enzyme catalysis and inhibitor binding affinity. While this information is very valuable for optimizing lead candidates, it also entails an enormous amount of time and manpower to prepare and characterize the analogues and site-directed mutants. Therefore, it is important to develop and validate computer aided drug design (CADD) methods that could help predict binding affinity changes between wild-type and mutants of thymidylate synthase.

To estimate the importance of hydrophobic residues to the binding affinity of MTX to TS, the following four mutations were carried out using FEP method: (i) $^{79}\text{Ile} : \text{MTX} \rightarrow ^{79}\text{Val} : \text{MTX}$ (ii) $^{79}\text{Ile} : \text{MTX} \rightarrow ^{79}\text{Ala} : \text{MTX}$ (iii) $^{79}\text{Ile} : \text{MTX} \rightarrow ^{79}\text{Leu} : \text{MTX}$, and (iv) $^{176}\text{Phe} : \text{MTX} \rightarrow ^{176}\text{Ile} : \text{MTX}$. These simulations examine the strength of the contribution of electrostatic (ΔG_{ele}) and van der Waals (ΔG_{vdW}) forces in the form of intra-molecular and inter-molecular components between the MTX and TS. The calculated and experimental binding free energy results of four different mutants are given in Table 1. The first three mutations are to understand the effect of replacing ^{79}Ile with **Val**, **Ala** and **Leu**. The shortest distance between C_{δ} of ^{79}Ile with any carbon of the phenyl ring in methotrexate is 3.82 Å. So, in the first mutation, a deletion of that carbon, (*i.e.*, replacing **Ile** with **Val**) is expected to have a minor change in the binding affinity. The relative binding free energy computed for the mutation $^{79}\text{Ile} \rightarrow ^{79}\text{Val}$ with MTX is 0.80 kcal mol⁻¹, which is consistent with our rationalization and the experimental value of 0.55 kcal mol⁻¹. A considerable loss in binding can be expected by the replacement of $^{79}\text{Ile} \rightarrow ^{79}\text{Ala}$ because of the loss of three methyl carbons which contribute to the hydrophobic interactions of the protein to the phenyl of MTX. The relative solvation free energy (ΔG_{sol}) for the mutation $^{79}\text{Ile} \rightarrow ^{79}\text{Ala}$ is -0.60 kcal mol⁻¹ and the relative binding free energy (ΔG_{bind}) is 1.80 kcal mol⁻¹, which is in good agreement with the experimental value of 1.40 kcal mol⁻¹. The third mutation in the series $^{79}\text{Ile} \rightarrow ^{79}\text{Leu}$ is interesting in view of the identical number of atoms for the reactant and product states. The computed relative binding free energy value (1.2 kcal mol⁻¹) for that mutation compares favorably with the experimental value of 1.0 kcal mol⁻¹. As shown in Table 1, in all three mutants the desolvation cost for **Ile** is less than other mutants. As a result, the loss of binding affinity for these mutants is a combination of both desolvation costs as well as a loss of hydrophobic interaction in the complex. It is notable that the calculated relative free energy difference arises from the van der Waals part of the free energy simulation. The order of hydrophobic interactions, **Ile** > **Val** > **Leu** > **Ala**, is consistent with calculated and experimental relative binding affinities of MTX with corresponding TS mutants. The calculated relative solvation and binding

affinity for fourth mutation, $^{176}\text{Phe} \rightarrow ^{176}\text{Ile}$, is 2.9 kcal mol⁻¹ and 1.7 kcal mol⁻¹ respectively, which is consistent with the experimental value of 1.2 kcal mol⁻¹. The desolvation cost (2.9 kcal mol⁻¹) of ^{176}Phe as compared to ^{176}Ile was compensated by good hydrophobic interactions of ^{176}Phe with MTX.

Conclusions

We have validated the FEP methodology for predicting binding affinities of thymidylate synthase mutants with methotrexate inhibitor. The results of the calculated relative free energies indicated that ^{79}Val , ^{79}Ala , ^{79}Leu and ^{176}Ile play an important role through hydrophobic interactions, which are affecting the binding affinity of methotrexate to thymidylate synthase. Any changes in these hydrophobic interactions due to mutations on the protein will have significant effect on the binding affinity of MTX to thymidylate synthase, particularly for the mutant of ^{176}Phe to ^{176}Ile . The solvation free energies and the relative binding affinities of the mutant residues showed that the hydrophobic interactions of methotrexate have an important role with the binding pocket of thymidylate synthase. These CADD methods will also have several applications from basic research applications to better drugs design. Understanding the binding pocket of a protein can allow a researcher to design potent drug candidates for a given drug target. Often people grow resistant to drugs, and one could use CADD methods for designing novel drugs when patients show resistance to the current drugs, such as for AIDS and cancer. Finally, this could potentially lead to designing novel inhibitors which could work with these new variants.

References

1. Matthews DA, Appelt K, Oatley SJ, Xuong NgH (1990) J Mol Biol 214:923–926
2. Jones T, Calvert A, Jackman AL, Eakin MA, Smithers MJ, Betteridge RF, Newell DR, Hayter AJ, Stocker A, Harland SJ, Davis LC, Harrap KR (1985) J Med Chem 28:1468–1476
3. Jones TR, Varney MD, Webber SE, Lewis KK, Marzoni GP, Palmer CL, Kathardekar V, Welsh KM, Webber S, Matthews DA, Appelt K, Smith WW, Janson CA, Villfranca JE, Bacquet RJ, Howland EF, Bartlett CA, Morse CA (1996) J Med Chem 39:904–917
4. Nair MG, Nanavati NT, Nair IG, Kialiuk RL, Gaumont Y, Hsiao MC, Kalman TI (1986) J Med Chem 29:1754–1760
5. Matthews DA, Villfranca JE, Janson CA, Smith WW, Welsh K, Freer S (1990) J Mol Biol 214:937–948
6. Liu L, Santi DV (1993) Biochem 32:9263–9267
7. Liu L, Santi DV (1992) Biochem 31:5010–5014
8. Appelt K, Bacquet RJ, Bartlett CA, Booth CL, Freer ST, Fuhry MAM, Gehring MR, Hermann SM, Howland EF, Janson CA, Jones TR, Kan C, Kathardekar V, Lewis KK, Marzoni GP,

- Matthews DA, Mohr C, Moomaw EW, Morse CA, Oatley SJ, Ogden RO, Reddy MR, Reich SH, Schoettlin WS, Smith WW, Varney MD, Villafranca JE, Ward RW, Webber SE, Welsh KM, White J (1991) *J Med Chem* 34:1925–1934
9. Holloway K, Wai JM, Halgren TA, Fitzgerald PM, Vacca JP, Dorsey BD, Levin RB, Thompson WJ, Chen JL, deSolms JS, Gaffin N, Ghosh AK, Giuliani EA, Graham SL, Guare JP, Hungate RW, Lyle TA, Sanders WM, Tucker TJ, Wiggins M, Wiscourt CM, Woltersdorf OW, Young SD, Darke PL, Zugay JA (1995) *J Med Chem* 38:305–317
 10. Varney MD, Appelt K, Kalish V, Reddy MR, Tatlock J, Palmer CL, Romies WH, Wu BW, Musick L (1994) *J Med Chem* 37:2274–2284
 11. Erion MD, Montgomery JA, Niwas S, Rose JD, Ananthan S, Allen M, Secrist JA, Babu SY, Bugg CE, Guida WC, Ealick SE (1993) *J Med Chem* 36:3771–3783
 12. Erion MD, Dang Q, Reddy MR, Rao KS, Huang J, Lipscomb WN, van Poelje PD (2007) *J Am Chem Soc* 129:15480–15490
 13. Dang Q, Rao KS, Reddy KR, Jiang T, Reddy MR, Potter SC, Fujitaki JM, van Poelje PD, Huang J, Lipscomb WN, Erion MD (2007) *J Am Chem Soc* 129:15491–15502
 14. Reddy MR, Erion MD, Agarwal A (2001) In: Lipkowitz KB and Boyd DB (eds) *Reviews in Computational Chemistry*, vol 16. Wiley, New York, NY, pp 217–304
 15. Reddy MR, Viswanadhan VN, Weinstein JN (1991) *Proc Natl Acad Sci USA* 88:10287–10291
 16. Ferguson DM, Radmer RJ, Kollman PA (1991) *J Med Chem* 34:2654–2659
 17. Tropshaw AJ, Hermans J (1999) *J Prot Eng* 5:29–33
 18. Rao BG, Tilton RF, Singh UC (1992) *J Am Chem Soc* 114:4447–4452
 19. Fleischman SH, Brooks CL (1990) *Proteins: Struct Funct and Genet* 7:52–61
 20. Merz KM, Kollman PA (1989) *J Am Chem Soc* 111:5649–5658
 21. Reddy MR, Varney MD, Kalish V, Viswanadhan VN, Appelt K (1994) *J Med Chem* 114:10117–10122
 22. Erion MD, van Poelje PD, Reddy MR (2000) *J Am Chem Soc* 122:6114–6115
 23. Reddy MR, Erion MD (2001) *J Am Chem Soc* 123:6246–6252
 24. Singh UC (1988) *Proc Natl Acad Sci* 85:4280–4284
 25. Reddy MR, Bacquet RJ, Zichi D, Matthews DA, Welsh KM, Jones TR, Freer S (1992) *J Am Chem Soc* 114:10117–10122
 26. Rastelli G, Thomas B, Kollman PA, Santi DV (1995) *J Am Chem Soc* 117:7213–7227
 27. Lee T-S, Kollman PA (2001) In: Reddy MR, Erion MD (eds) *Free Energy Calculations in Rational Drug Design*. Kluwer, New York, NY, pp 335–343
 28. Ravichandra Mutyala, Reddy RN, Sumakanth M, Reddanna P, Reddy MR (2007) *J Comp Chem* 28:932–937
 29. *Galaxy Molecular Modeling Software and AM2000 Macromolecular Simulation package* (1995) AM Technologies, Inc. San Antonio, TX, Copyright
 30. Weiner SJ, Kollman PA, Case DA, Singh UC, Ghio C, Alagoha G, Profeta S Jr, Weiner PK (1984) *J Am Chem Soc* 106:765–784
 31. Singh UC, Weiner PK, Caldwell JK, Kollman PA (1986) *AMBER version 3.0*. University of California at San Francisco
 32. Berendsen HJC, Grigera JR, Straatsma TP (1987) *J Phys Chem* 91:6269–6271
 33. Reddy MR, Berkowitz M (1989) *Chem Phys Lett* 155:173–176
 34. Frisch MJ, Head-Gordon HB, Schlegel K, Raghavachari JS, Binkley C, Gonzalez DJ, Defrees DJ, Fox RJ, Whiteside R, Seeger CF, Melius J, Baker R, Martin LR, Kahn JJP, Stewart EM, Fluder S, Topiol JA, Pople JA (1994) *Gaussian Inc*, Pittsburgh, PA
 35. Chirlian LE, Francl MM (1987) *J Comp Chem* 8:894–905
 36. Verlet L (1967) *Phys Rev* 159:98–103
 37. Ryckaert JP, Ciccotti G, Berendsen HJC (1977) *J Comp Phys* 23:327–341